

# Quasar H II Regions During Cosmic Reionization

Marcelo A. Alvarez<sup>†</sup> and Tom Abel

*Kavli Institute for Particle Astrophysics and Cosmology, Stanford University, Stanford, CA 94305*

26 May 2019

## ABSTRACT

Cosmic reionization progresses as H II regions form around sources of ionizing radiation. Their average size grows continuously until they percolate and complete reionization. We demonstrate how this typical growth can be calculated around the largest, biased sources of UV emission such as quasars by further developing an analytical model based on the excursion set formalism. This approach allows us to calculate the sizes and growth of the HII regions created by the progenitors of any dark matter halo of given mass and redshift with a minimum of free parameters. Statistical variations in the size of these pre-existing HII regions are an additional source of uncertainty in the determination of very high redshift quasar properties from their observed HII region sizes. We use this model to demonstrate that the transmission gaps seen in very high redshift quasars can be understood from the radiation of only their progenitors and associated clustered small galaxies. The fit requires the epoch of overlap to be at  $z = 5.8 \pm 0.1$ . This interpretation makes the transmission gaps independent of the age of the quasars observed. If this interpretation were correct it would raise the prospects of using radio interferometers currently under construction to detect the epoch of reionization.

**Key words:** galaxies:formation–quasars–intergalactic medium–cosmology:theory – reionization

## 1 INTRODUCTION

Recent observations are just beginning to reveal the epoch of cosmological reionization, which defines a fundamental transition in the universe, separating the cosmic dark ages (e.g. Rees 1998) from the epoch of galaxy formation and evolution. The appearance of a Gunn-Peterson trough (Gunn & Peterson 1965) in quasar spectra indicates that reionization was ending at  $z \sim 6$  (e.g. Becker et al. 2001; Fan et al. 2002; White et al. 2003), while the large-angle polarization anisotropy of the cosmic microwave background observed by the Wilkinson Microwave Anisotropy Probe (Spergel et al. 2006) indicates the universe may have been significantly reionized by  $z \sim 10$  (Page et al. 2006). Observations of Lyman- $\alpha$  emitting galaxies at  $z \sim 5 - 7$  are posing puzzles with regard to the reionization history at those redshifts (e.g. Haiman 2002; Hu et al. 2002; Malhotra & Rhoads 2004). These and other current and future observations pose several important questions and constraints for the theory of reionization.

In order to answer these questions much theoretical effort is underway. Numerical studies have provided insights into the asymmetric nature of ionization fronts (Abel, Norman & Madau 1999; Ciardi et al. 2001; Alvarez, Bromm, & Shapiro 2006), radiative feedback (Ricotti, Gnedin, & Shull 2002; Shapiro, Iliev, & Raga 2004; Whalen, Abel, & Norman 2004; Kitayama et al. 2004; Abel, Wise, & Bryan 2006; Susa & Umemura 2006; Ahn &

Shapiro 2007), the reionization history (Gnedin & Ostriker 1999; Ciardi, Ferrara, & White 2003; Sokasian et al. 2004), and the large-scale structure of reionization (Iliev et al. 2006a; Zahn et al. 2006; Kohler, Gnedin, & Hamilton 2005). Because of practical limitations, numerical studies are expensive and it is difficult to know which processes to simulate directly and which to parameterize. Analytical studies can play a complementary role. The earliest studies of reionization were almost exclusively analytical. Most modeled reionization by considering the growth of H II regions around sources of ionizing radiation in a homogeneous expanding universe with a clumping factor (e.g. Shapiro & Giroux 1987). While simplistic, models based on this assumption have proved valuable (e.g. Haiman & Loeb 1997; Madau, Haardt, & Rees 1999; Haiman & Holder 2003; Iliev, Scannapieco, & Shapiro 2005). Studies that describe the thermodynamics of the IGM during reionization have added additional affects such as non-equilibrium ionization and heating and an evolving UV background (e.g. Arons & Wingert 1972; Shapiro, Giroux, & Babul 1994; Miralda-Escude & Rees 1994; Hui & Gnedin 1997; Miralda-Escude, Haehnelt, & Rees 2000; Hui & Haiman 2003; Choudhury & Ferrara 2005).

In order to understand the very large scale structure of reionization, analytical models for the sizes H II regions during reionization have recently been developed (Wyithe & Loeb 2004b; Furlanetto, Zaldarriaga, & Hernquist 2004 – hereafter FZH04; Furlanetto & Oh 2005; Furlanetto, McQuinn, & Hernquist 2006; Wyithe & Loeb 2006; Cohn & Chang 2007). For example, FZH04 found that typical H II region sizes during reionization were 1–10 Mpc.

<sup>†</sup> e-mail: malvarez@slac.stanford.edu

## 2 Alvarez & Abel

These predictions were qualitatively verified by the radiative transfer simulations of Zahn et al. (2006). While they did not directly compare their simulations to the analytical predictions, they did develop a ‘‘hybrid’’ technique and showed that it gives strikingly similar results to their radiative transfer simulations. The FZH04 model has been used to predict the 21-cm background (McQuinn et al. 2006) as well as the kinetic Sunyaev Zel’dovich effect (McQuinn et al. 2005). Furlanetto, Zaldarriaga, & Hernquist (2006) used it to make predictions for the effects of reionization on Ly $\alpha$  galaxy surveys, while Dijkstra, Wyithe, & Haiman (2006) used it to provide a lower limit to the ionized fraction at  $z = 6.5$ . Kramer, Haiman, & Oh (2006) extended the FZH04 model to include the effects of clustering and feedback on the size distribution, the former of which we will address analytically here. Alvarez et al. (2006) used the model to estimate the cross-correlation between the cosmic microwave and 21-cm backgrounds on large scales.

Observational detection of individual H II regions and measurement of their sizes would provide strong constraints on the sources responsible for reionization. Until now, such detection has remained elusive, due to complexities in the interpretation of quasar spectra. These difficulties arise in the interpretation of the ‘‘transmission gap’’ between the quasar’s Ly $\alpha$  line and the onset of the Gunn-Peterson trough. This gap has been interpreted as corresponding to the quasar’s own H II region (e.g., Mesinger & Haiman 2004; Wyithe & Loeb 2004a). Alternatively the gap may be determined by a combination of the luminosity of the quasar and the UV radiation field – the Gunn-Peterson trough sets in whenever the flux from the quasar cannot keep the IGM sufficiently ionized (e.g., Yu & Lu 2005; Fan et al. 2006; Bolton & Haehnelt 2006; Mesinger & Haiman 2006). In this case, the H II region could be much larger than the size corresponding to the transmission gap, but it obviously could not be smaller. Wyithe & Loeb (2004b) discussed the effect of the size distribution of bubbles on the scatter in the epoch of overlap, but did not address the issue of the transmission gap. Furlanetto & Oh (2005) also addressed the issue of the bubble sizes near overlap, paying particular attention to the role of recombinations on the mean free path of ionizing photons, while Lidz, Oh, & Furlanetto (2006), Bolton & Haehnelt (2007), and Maselli et al. (2007) examined the effects on quasar spectra due to density fluctuations in the IGM.

Here we will model the size of pre-existing HII regions that existed around these high redshift quasars before they began to shine. We will characterize them by using the conditional H II region size distribution, which describes statistically the size distribution of H II regions that surround haloes of a given mass. In §2 we review the model and derive the conditional bubble distribution. In §3 we discuss the implications for quasar H II regions, and conclude with a summary and discussion in §4. We adopt parameters based on WMAP 3-year observations (Spergel et al. 2006),  $(\Omega_m h^2, \Omega_b h^2, h, n_s, \sigma_8) = (0.13, 0.022, 0.73, 0.95, 0.74)$ .

## 2 CONDITIONAL H II REGION SIZES

In the model of FZH04, the size of the H II region in which a point lies is determined by finding the largest spherical region centered on the point for which the mean collapsed fraction  $f_{\text{coll}} > \zeta^{-1}$ , where  $\zeta$  is an efficiency parameter which describes how many ionizing photons are produced per collapsed atom. By using the extended Press-Schechter formalism, they showed that this condition can be expressed in terms of the mean overdensity of the region,  $\delta_m$ , by

$$\delta_m \geq \delta_x(m, z) \equiv \delta_c(z) - \sqrt{2}K(\zeta) [\sigma_{\min}^2 - \sigma^2(m)]^{1/2}, \quad (1)$$

where  $m$  is the mass of the region,  $\sigma^2(m)$  is the variance of density fluctuations on that scale,  $\delta_c(z)$  is the critical density for collapse, and  $\sigma_{\min}^2 \equiv \sigma^2(m_{\min})$  is the variance on the scale of the minimum halo mass which contributes to reionization,  $m_{\min}$ .<sup>1</sup> By finding a linear approximation to the ‘‘barrier’’,

$$\delta_x(m, z) \simeq B(m, z) \equiv B_0(z) + B_1(z)\sigma^2(m), \quad (2)$$

where

$$B_0(z) = \delta_c - \sqrt{2}K(\zeta)\sigma_{\min}, \quad B_1(z) = \frac{K(\zeta)}{\sqrt{2}\sigma_{\min}}, \quad (3)$$

and  $K(\zeta) = \text{erf}^{-1}(1 - \zeta^{-1})$ , they were able to derive the mass function of ionized regions,

$$M_b \frac{dn}{dM_b} = \sqrt{\frac{2}{\pi}} \frac{\rho}{M_b} \left| \frac{d \ln \sigma}{d \ln M_b} \right| \frac{B_0}{\sigma(M_b)} \exp \left[ -\frac{B^2(M_b, z)}{2\sigma^2(M_b)} \right]. \quad (4)$$

Additional details can be found in FZH04.

What is the probability,  $f(M_b|M)dM_b$ , that a halo of mass  $M$  will be located in an ionized bubble with a size between  $M_b$  and  $M_b + dM_b$ ? This can be found by considering the halo to be the locus of the first upcrossing of a random walk in  $\delta$ . For the barrier used by FZH04,  $B(M, z) < \delta_c$  for  $\sigma(M) < 2\sigma_{\min}$ .

First, we determine the conditional probability,  $f(S, \delta_c|S_b, \delta_b)dS$ , that a point which first crossed the barrier at  $S_b \equiv \sigma^2(M_b)$  and  $\delta_b \equiv B(M_b, z)$ , crosses the halo barrier  $\delta_c$  between  $S \equiv \sigma^2(M_h)$  and  $S + dS$ . As has been discussed previously (e.g. Sheth 1998), this can be accomplished by using the standard expression for the distribution of up-crossings of a linear barrier for trajectories starting from  $S = 0$  and  $\delta = 0$ ,

$$f(S, \delta_c|0, 0)dS = \frac{\delta_c}{\sqrt{2\pi S}} \exp \left[ -\frac{\delta_c^2}{2S} \right] \frac{dS}{S}, \quad (5)$$

but moving the origin to  $(S_b, \delta_b)$  (see also Furlanetto et al. 2006, equation 2),

$$f(S, \delta_c|S_b, \delta_b)dS = \frac{\delta_c - \delta_b}{\sqrt{2\pi}(S - S_b)^{3/2}} \exp \left[ -\frac{(\delta_c - \delta_b)^2}{2(S - S_b)} \right] dS. \quad (6)$$

The conditional probability that the first up-crossing of the bubble barrier occurred between  $S_b$  and  $S_b + dS_b$ , given that it crosses the halo barrier  $\delta_c$  at  $S > S_b$ , is

$$f(S_b, \delta_b|S, \delta_c)dS_b = \frac{f(S_b, \delta_b|0, 0)}{f(S, \delta_c|0, 0)} f(S, \delta_c|S_b, \delta_b)dS_b. \quad (7)$$

Thus, the probability that a halo of mass  $M$  is inside an ionized bubble of mass between  $M_b$  and  $M_b + dM_b$  is

$$f(M_b|M)dM_b = f(S_b, \delta_b|S, \delta_c) \frac{dS_b}{dM_b} dM_b \quad (8)$$

$$= \frac{1}{\sqrt{2\pi}} \frac{B_0}{\delta_c} \left[ \frac{S}{S_b(S - S_b)} \right]^{3/2} \left| \frac{dS_b}{dM_b} \right| \times \quad (9)$$

$$\exp \left\{ \frac{\delta_c^2}{2S} - \frac{\delta_b^2}{2S_b} - \frac{[\delta_c - \delta_b]^2}{2(S - S_b)} \right\} dM_b. \quad (10)$$

<sup>1</sup> We will use the convention in which  $\delta_c(z)$  is a function of redshift, while  $\sigma^2(m)$  is always the variance evaluated at present. We will also suppress the explicit  $z$ -dependence in our notation, so that  $\delta_c \equiv \delta_c(z)$ .

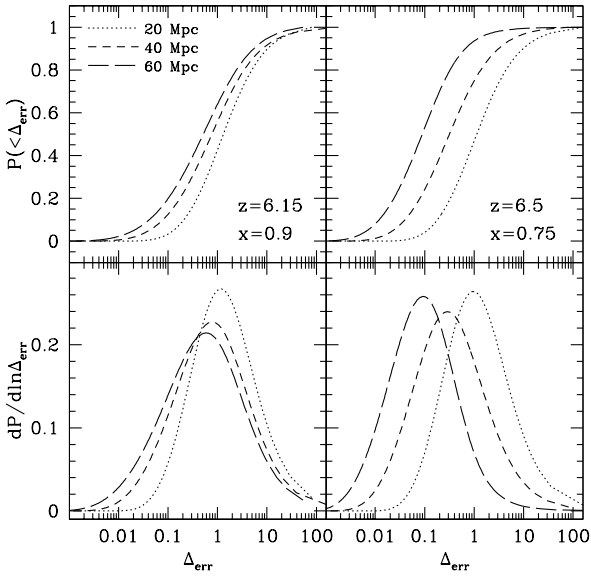


**Figure 1.** Distribution of number of photons produced by the quasar,  $N_{\text{tot}}$ , for a given observed comoving H II region radius,  $R_{\text{obs}} = 20$  Mpc (dotted), 40 Mpc (dashed), 60 Mpc (long dashed), 80 Mpc (dot-dashed). Both models are for a minimum halo virial temperature of  $T_{\text{min}} = 10^4$  K.

### 3 QUASAR H II REGIONS

In this section we will discuss the implications of the conditional H II region size distribution on observations of quasar H II regions. Before proceeding, we briefly describe what we mean by quasar H II region, especially near the end of reionization.

Late in reionization, close to percolation, the H II region sizes grow rapidly. This is of course the expected behaviour, but it is not clear what meaning to attach to any given H II region when most of the universe is already ionized. For H II regions around very rare quasar host halos, it is reasonable to expect that the central H II region in which the quasar forms is much larger than the surrounding H II regions. While the mean global ionized fraction may be high, the fluctuations in ionized fraction outside of the central H II region are likely to be on much smaller scales.

#### 3.1 Interpretation of observed H II region sizes

The variation in the size of *pre-existing* H II regions that surround quasars when they begin to shine manifests itself in a theoretical uncertainty in the determination of properties of quasars, such as their ionizing photon luminosity and age, as well as properties of the surrounding medium, such as the neutral fraction and gas density. For a quasar that has been on for a time  $t$  and has an ionizing photon luminosity  $\dot{N}_\gamma$ , the observed line-of-sight radius of its H II region,  $R_{\text{obs}}$ , is related to the radius of the H II region in which it initially lies,  $R_b$ , by

$$\frac{\dot{N}_\gamma t}{(1-x)n_H} \equiv V = \frac{4\pi}{3} (R_{\text{obs}}^3 - R_b^3) = V_0 (1 - R_b^3/R_{\text{obs}}^3) \quad (11)$$

where  $V_0 \equiv 4\pi R_{\text{obs}}^3/3$  is the volume contained within if the quasar had begun to emit with no pre-existing H II region ( $R_b = 0$ ),  $n_H$  is the hydrogen number density,  $x$  is the ionized fraction, and we have assumed  $t < t_{\text{rec}} = 1.9$  Gyr  $C_l^{-1}(1+\delta)^{-1}[(1+z)/7]^{-3}$ , where  $C_l$  is the clumping factor. The quantity  $V$  is the volume that is

actually ionized by the quasar itself, *excluding* the volume already ionized by existing nearby sources,  $V_0$ .

What is the uncertainty in the determination of  $V$ , given that the initial radius of the H II region,  $R_b$ , is unknown? We express this uncertainty in terms of an error

$$\Delta_{\text{err}} \equiv \frac{V_0 - V}{V}, \quad (12)$$

which is the fractional amount by which the uniform-IGM estimate for the volume ionized by the quasar,  $V_0$ , exceeds the actual one,  $V$ . We obtain

$$\frac{dP}{d\ln\Delta_{\text{err}}} = \frac{1 - R_b^3/R_{\text{obs}}^3}{3(2 - R_b^3/R_{\text{obs}}^3)} \frac{dP}{d\ln R_b}. \quad (13)$$

This distribution is shown in Figure 1 for different values of  $R_{\text{obs}}$ . For larger observed H II regions, the overestimate of  $V$  is smaller. If the ionizing luminosity and age of the quasar are known, as well as the density of the surrounding gas, then the neutral fraction can be determined according to

$$1 - x \equiv x_{\text{HI}} = \frac{\dot{N}_\gamma t}{n_H V}. \quad (14)$$

Of course, the luminosity, age, and density are not known exactly, but arguments can be made based upon their likely values (e.g. Wyithe & Loeb 2004). The error in  $V$  is related to an error in  $x_{\text{HI}}$  by  $x_{\text{HI}}/x_{\text{HI},0} = 1 + \Delta_{\text{err}}$ . Since  $\Delta_{\text{err}} > 0$ , the neutral fraction is always underestimated when the presence of existing H II regions is not taken into account. There are therefore two reasons why higher neutral fractions lead to smaller H II regions. First, higher neutral fractions lead to slower ionization fronts propagating away from the quasar and thus to smaller H II regions. Second, the higher the neutral fraction, the smaller the pre-existing H II region, which also leads to a smaller observed H II region.

#### 3.2 Proximity zones in quasar spectra

It has proven difficult to measure the sizes of H II regions around quasars directly, due to complexities in the interpretation of transmission gaps in their spectra. For example, Fan et al. (2006) define “proximity zones” as regions where the transmission is greater than ten percent, but do not explicitly associate them with the size of the quasar’s H II region. They found that these proximity zones have radii which increase steeply over the range  $6.4 \gtrsim z \gtrsim 5.8$ , from  $R_p \simeq 30$  to  $R_p \simeq 80$  comoving Mpc (Fig. 3). These values are similar to the size of H II regions around  $10^{12} M_\odot$  halos (a likely minimum value for the host halo masses of observed quasars at  $z \sim 6$ ; e.g. Volonteri & Rees 2006; Li et al. 2006) near the end of reionization (Fig. 2).

Shown also in Figure 3 is the evolution in the typical size of H II regions surrounding halos with masses  $\gtrsim 10^{12} M_\odot$  for a model in which the ionized fraction reaches unity at  $z_{\text{ov}} = 5.8$  and the integrated Thomson scattering optical depth (assuming once ionized helium) is  $\tau_{\text{es}} \simeq 0.055$ . The theoretical expectation for the evolution H II region sizes agrees quite well with the measured proximity zone sizes. This suggests that the evolving sizes of the proximity zones measured by Fan et al. (2006) can be explained by the growth of cosmic H II regions driven by clustered sources around the quasars alone. Taking into account the contribution from the quasars could change the theoretical prediction, since the flux contributed by the quasar at distances greater than the size of the pre-existing bubble may be large enough to increase transmission there. For a quasar with a spectral shape  $L_\nu \propto \nu^{-1.5}$  (e.g., Bolton &

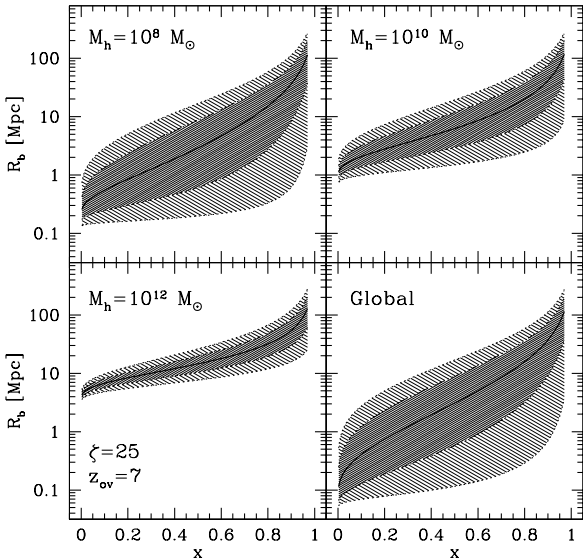


**Figure 2.** Shown is the evolution of the median bubble size (solid), along with the 68% (dark shaded region) and 95% (light shaded region) contours of the distribution. The “Global” panel is for the unconditional mean distribution, while the other panels are the conditional distributions given that the H II regions surround halos of total mass  $M_h$ , as labelled.

Haenelt 2007) and ionizing photon luminosity  $\dot{N}$ , ionization equilibrium implies that the neutral fraction at a comoving distance  $R$  is

$$f_{\text{HI}} \approx 4 \times 10^{-6} \left( \frac{c_l}{10} \right) \left( \frac{R}{38 \text{ Mpc}} \right)^2 \left( \frac{\dot{N}}{2 \times 10^{57} \text{ s}^{-1}} \right)^{-1}, \quad (15)$$

while the neutral fraction necessary to obtain a Gunn-Peterson optical depth  $\tau_{\text{GP}}$  is given by (Fan et al. 2006)

$$f_{\text{HI}} \approx 4 \times 10^{-6} \left( \frac{\tau_{\text{GP}}}{2} \right) \left( \frac{1+z}{7} \right)^{-3/2}. \quad (16)$$

For reasonable IGM clumping factors and quasar ionizing photon luminosities, therefore, the quasar by itself is able to cause transmission at a distance of 40 comoving Mpc, very similar to the size of the transmission gap in the highest redshift quasars measured by Fan et al. (2006). Thus, there are two possible explanations for the rapid increase in the size of the transmission gaps: 1) HII regions, defined as regions where hydrogen is mostly ionized, are much larger than the observed transmission gaps at  $z < 6.4$ . The transmission gaps correspond to smaller regions, within which the evolving UV intensity from a combination of nearby galaxies and the quasar ionizes the IGM to a level sufficient to allow transmission, or 2) The transmission gaps correspond to the extent of the HII regions themselves, which grow rapidly as overlap takes place at  $z \sim 6$ . The UV background intensity within these HII regions is dominated by galaxies clustered around the central quasar and is sufficient to cause the observed transmission.

#### 4 DISCUSSION

We have used the conditional H II region size distribution around halos with a mass  $\approx 10^{12} M_\odot$  to model observations of quasar H II regions. Our results can be summarized as follows:

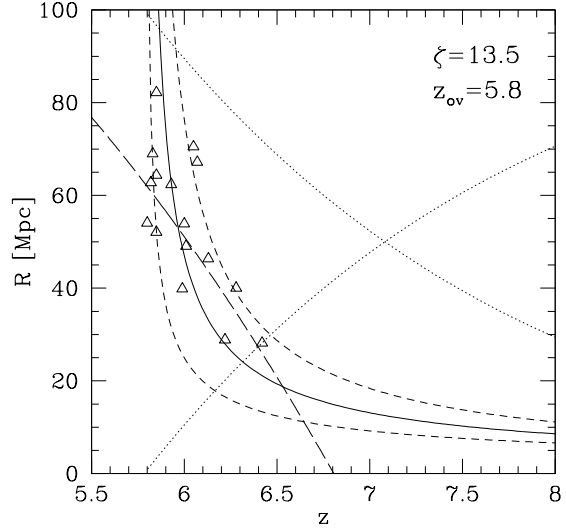


**Figure 3.** Median (solid) and 68% contours (dashed) of the size of H II regions surrounding a  $10^{12} M_\odot$  halo as a function of redshift for a model with  $\zeta = 13.5$  and  $z_{\text{ov}} = 5.8$ . Also shown are the “proximity zone” radii (triangles) of sixteen quasars as determined by Fan et al. (2006). The dotted lines are the ionized and neutral fractions multiplied by 100. Shown also is a linear fit (long dashed) of the proper size of the proximity regions vs. redshift, as in Fan et al. (2006).

1. Due to the biased location of quasars, the H II regions that surround them just before they begin to emit ionizing radiation are likely to be substantial, with radii of order tens of Mpc, even when the mean ionized fraction is of order thirty percent.

2. For observed quasar H II regions with sizes of order tens of Mpc, it is difficult to determine the intrinsic properties of the quasar and surrounding medium, due to uncertainties in the size of pre-existing H II regions. In general, neutral fractions will be underestimated while quasar luminosities and lifetimes will be overestimated (for a given density field – inhomogeneities can give the opposite effect, as in Bolton & Haehnelt 2007; Maselli et al. 2007). This effect is strongest for small observed H II regions around quasars late in the reionization epoch.

3. The observed transmission gaps around high-redshift quasars may have a direct correspondence to cosmic H II regions created by galaxies clustered around the central quasar. The steep increase in the transmission gap size at  $z < 6.4$  can be explained by the rapid growth of these H II regions at the epoch of overlap.

We expect conclusions (1) and (2) to be generally true, while for (3) to be the case, it is necessary for the UV radiation field within ionized bubbles to be sufficient to keep the volume-averaged neutral fraction low enough to create the observed transmission gaps. This is certainly plausible, since the UV radiation field near quasars is likely enhanced due to their biased environment (e.g., Yu & Lu 2005), with a size approaching that of the mean free path imposed by Lyman-limit systems ( $\sim 50$  comoving Mpc at  $z \sim 6$ ; Gnedin & Fan 2006).

There have been recent suggestions that detection of large ( $\sim 50$  comoving Mpc) H II regions by 21-cm tomography can reveal the locations of quasars and bright galaxies that just underwent an AGN phase (Wyithe, Loeb & Barnes 2005; Kohler et al. 2005). Our results here suggest that large, distinct H II regions may be visible at relatively low redshifts,  $z \sim 7$ , where foreground contam-

ination of the 21-cm observations is expected to be lowest. Thus, the 21-cm observations hold the most promise for discriminating between the two possible explanations for the evolution of transmission gap sizes discussed here. In addition, measurement of the sizes of H II regions around bright quasars by 21-cm tomography, when combined with the conditional H II region size distribution, will provide powerful constraints on the theory of reionization and the nature of high-redshift quasars.

In our model the global ionized fraction is proportional to the collapsed fraction, so that the same ionizing efficiency is assigned to collapsed matter, regardless of halo mass, epoch, or environment. In such a model, the ionized fraction grows exponentially with time. The reionization history is likely to be more complex than this, especially in light of the optical depth measured by WMAP. For example, self-regulated reionization, in which the lowest mass objects do not produce ionizing photons when they form within existing H II regions, can extend the reionization epoch, relieving the tension between a percolation at  $z \sim 6$  and the WMAP value of  $\tau_{\text{es}} \simeq 0.09$  (Haiman & Bryan 2006; Iliev et al. 2006b). We note, however, that our best-fitting model to the evolution of the transmission gap sizes, in which overlap is complete at  $z \simeq 5.8$  and  $\tau_{\text{es}} \simeq 0.055$ , is in marginal agreement with the value obtained from WMAP 3 year polarization data,  $\tau_{\text{es}} = 0.088^{+0.028}_{-0.034}$  (Spergel et al. 2006). This indicates that the level of early reionization demanded by the WMAP measurement may be quite modest, while still allowing for a late overlap at  $z = 5.8$ .

The fact that H II regions are likely to surround quasars before they begin to shine, and that the size of these regions will have a strong redshift dependence, are likely to be crucial in developing a more complete understanding of observations of the high redshift universe.

## ACKNOWLEDGMENTS

We wish to thank Zoltan Haiman and Peng Oh for a careful reading of an early draft, and Xiaohui Fan and Miguel Morales for helpful discussion. This work was partially supported by NSF CAREER award AST-0239709 from the National Science Foundation.

## REFERENCES

Abel T., Norman M.L., Madau P., 1999, *ApJ*, 523, 66  
 Abel T., Wise J.H., Bryan G.L., 2006, *ApJ*, submitted, astro-ph/0606019  
 Ahn K., Shapiro P.R., 2007, *MNRAS*, 375, 881  
 Alvarez M.A., Bromm V., Shapiro P.R., 2006, *ApJ*, 639, 621  
 Alvarez M.A., Komatsu E., Doré O., Shapiro P.R., 2006, *ApJ*, 647, 840  
 Arons J., Wingert D.W. 1972, *ApJ*, 177, 1  
 Becker, R. H., et al. 2001, *AJ*, 122, 2850  
 Bolton J.S., Haehnelt M.G., 2007, *MNRAS*, 374, 493  
 Choudhury T.R., Ferrara A., 2005, *MNRAS*, 361, 577  
 Choudhury T.R., Ferrara A., 2006, *MNRAS*, 371L, 55  
 Ciardi B., Ferrara A., Marri S., Raimondo G., 2001, *MNRAS*, 324, 381  
 Ciardi B., Ferrara A., White S.D.M., 2003, *MNRAS*, 344L, 7  
 Cohn J.D., Chang T., 2007, *MNRAS*, 374, 72  
 Dijkstra M., Lidz A., Wyithe S., 2007, *MNRAS*, submitted, astro-ph/0701667  
 Dijkstra M., Wyithe S., & Haiman Z., 2006, *MNRAS*, submitted, astro-ph/0611195  
 Fan X., et al., 2002, *AJ*, 123, 1247  
 Furlanetto S.R., Oh, S.P., 2005, *MNRAS*, 363, 1031  
 Furlanetto S. R., Zaldarriaga M., Hernquist L., 2004, *ApJ*, 613, 1  
 Furlanetto S.R., Zaldarriaga M., Hernquist L., 2006, *MNRAS*, 365, 1012  
 Furlanetto S. R., McQuinn M. & Hernquist L., 2006, *MNRAS*, 365, 115  
 Gnedin N. Y., Ostriker J.P., 1999, *ApJ*, 486, 581  
 Gnedin N. Y., Fan, X., 2006, *ApJ*, 648, 1  
 Gunn, J. E., Peterson, B. A., 1965, *ApJ*, 142, 1633  
 Haiman, Z., 2002, *ApJ*, 576, 1  
 Haiman Z., Loeb, A. 1997, *ApJ*, 483, 21  
 Haiman Z., Holder G.P., 2003, *ApJ*, 595, 1  
 Haiman Z., Bryan G.L., 2006, *ApJ*, 650, 27  
 Hu E.M., et al., 2002, *ApJ*, 568, L75  
 Hui L., Gnedin N.Y., 1997, *MNRAS*, 292, 27  
 Hui L., Haiman Z., 2003, *ApJ*, 596, 9  
 Iliev I. T., Scannapieco E., Shapiro P. R., 2005, *ApJ*, 624, 491  
 Iliev I.T., Mellema G., Pen U.-L., Merz H., Shapiro P.R., Alvarez M.A., 2006a, *MNRAS*, 369, 1625  
 Iliev I. T., Mellema G., Shapiro P. R., and Pen, U., 2006b, *MNRAS*, submitted (astro-ph/0607517)  
 Kitayama T., Yoshida N., Susa H., & Umemura M., 2004, *ApJ*, 613, 631  
 Kohler K., Gnedin N. Y., Hamilton A. J. S., 2005, astro-ph/0511627)  
 Kohler K., Gnedin N. Y., Miralda-Escudé J., Shaver P. A., 2005, *ApJ*, 633, 552  
 Kramer R.H., Haiman Z., Oh S.P., 2006, *ApJ*, 649, 570  
 Li Y., et al., 2006, *ApJ*, submitted, astro-ph/0608190  
 Lidz A., Oh S.P., Furlanetto S.R., 2006, *ApJ*, 639, L47  
 Madau P., Haardt F., Rees M.J., 1999, *ApJ*, 514, 648  
 Malhotra S., Rhoads J. E., 2004, *ApJ*, 617, L5  
 Maselli A., Gallerani S., Ferrara A., Choudhury T.R., 2007, *MNRAS*, in press, astro-ph/0608209  
 McQuinn M., Furlanetto S. R., Hernquist L., Zahn O., Zaldarriaga M., 2005, *ApJ*, 630, 643  
 McQuinn M., Zahn O., Zaldarriaga M., Hernquist L., Furlanetto S.R., 2006, *ApJ*, 653, 815  
 Mesinger A., Haiman Z., 2004, *ApJ*, 613, 23  
 Mellema G., Iliev I. T., Pen U. L., Shapiro P. R., 2006, *MNRAS*, submitted (astro-ph/0603518)  
 Miralda-Escude J. & Rees M.J., 1994, *MNRAS*, 266, 343  
 Miralda-Escude J., Haehnelt, M., Rees M.J., 2000, *ApJ*, 530, 1  
 Page et al., 2006, *ApJ*, submitted, astro-ph/0603450  
 Press W. H., Schechter P., 1974, *ApJ*, 187, 425  
 Rees M.J., 1997, in Tanvir N.R., Aragon-Salamanca A., Wall J.V., eds., *The Hubble Space Telescope and the High Redshift Universe*. World Scientific, Singapore, p. 115  
 Ricotti M., Gnedin N.Y., & Shull M.J., 2002, *ApJ*, 575, 49  
 Ricotti M. & Ostriker J. P., 2004, *MNRAS*, 352, 547  
 Shapiro P. R., Giroux M. L., 1987, *ApJ*, 321, L107  
 Shapiro P. R., Giroux M. L., Babul A., 1994, *ApJ*, 427, 25  
 Shapiro P. R., Iliev I. T., Raga A. C., 2004, *MNRAS*, 348, 753  
 Sokasian A., Yoshida N., Abel T., Hernquist L., Springel V., 2004, *MNRAS*, 350, 47  
 Spergel D.N., et al., 2006, *ApJ*, submitted (astro-ph/0603449)  
 Susa H. & Umemura M., 2006, *ApJ*, 645, L93  
 Volonteri M., Rees M.J., 2006, *ApJ*, 650, 669  
 Whalen D., Abel T., & Norman M., 2004, *ApJ*, 610, 14  
 White R.L., Becker R.H., Fan X., Strauss M.A., 2003, *AJ*, 126, 1  
 Wyithe J.S.B., Loeb A., 2004a, *Nature*, 427, 815  
 Wyithe J.S.B., Loeb A., 2004b, *Nature*, 432, 194

Wyithe J.S.B., Loeb A., 2006, MNRAS, submitted, astro-ph/0609734

Wyithe J.S.B., Loeb A., Barnes D.G., 2005, ApJ, 634, 715

Yu Q., & Lu Y., 2005, ApJ, 620, 31

Zahn O. et al. 2006, ApJ, submitted (astro-ph/0604177)

Zaldarriaga M., Furlanetto S., & Hernquist L., 2004, ApJ, 608, 622

Zahn, O. et al., 2007, ApJ, 2007, 654, 12